

## Surface Priming and the Self-Assembly of Hydrogen-Bonded Multilayer Capsules and Films

Veronika Kozlovskaya, Sergey Yakovlev, Matthew Libera, and Svetlana A. Sukhishvili\*

*Department of Chemistry and Chemical Biology, Stevens Institute of Technology, Hoboken, New Jersey 07030*

*Received January 28, 2005; Revised Manuscript Received March 8, 2005*

**ABSTRACT:** We present a systematic study of how growth of hydrogen-bonded multilayers is affected by the substrate shape and charge as well as by the deposition conditions of a polycation precursor layer. We contrast growth of strongly bound poly(*N*-vinylpyrrolidone)/poly(methacrylic acid) (PVPON/PMAA) and weakly bound poly(ethylene oxide)/poly(methacrylic acid) (PEO/PMAA) systems when these multilayers are deposited onto bare or poly(ethylene imine) (PEI)-treated surfaces of CdCO<sub>3</sub> crystals, colloidal silica particles, or silicon wafers. As compared to flat substrates, growth of hydrogen-bonded multilayers was significantly inhibited when colloidal particles were used as a substrate, presumably due to the enhanced chain removal by shaking the particulate substrate during the polymer adsorption. While in the PVPON/PMAA system robust multilayer deposition occurred on the precursor-treated substrate regardless of the adsorption history of the precursor layer, growth of PEO/PMAA films was critically dependent on the conditions of PEI adsorption. PEO/PMAA films could be grown on CdCO<sub>3</sub> substrates when the PEI precursor was allowed to adsorb at a pH value higher than that used for hydrogen-bonding deposition, but PEO/PMAA film growth was inhibited when PEI was deposited at the same pH used for film deposition. We rationalize this effect in terms of the role the precursor layer plays on the growth of hydrogen-bonded multilayers, and we confirm our hypothesis by monitoring electrophoretic mobility, ionization, and the amount of polymer deposited within the precursor layer. Finally, we suggest two ways to facilitate growth of hydrogen-bonded multilayers onto substrates which carry unfavorably high negative charge: construction of hybrid hydrogen-bonded multilayers and the use of divalent cations as promoters of PMAA binding.

### Introduction

The deposition of organic polymers at surfaces via layer-by-layer sequential adsorption presents a powerful tool for surface modification and fabrication of polymer films of controlled thickness. Though electrostatic self-assembly has largely been used to produce surface-mediated self-assembled polymer films,<sup>1</sup> hydrogen bonding has been recently explored as an attractive means to govern polymeric deposition at surfaces.<sup>2–5</sup> One type of hydrogen-bonded self-assembly involves polymers from aqueous solutions and yields films which can be erased by an increase in solution acidity toward a more neutral value.<sup>4,6</sup> We have also recently shown that hydrogen-bonded polymers of the latter type can be deposited onto particulate substrates, in a way similar to earlier known electrostatically self-assembled polymers, producing pH-responsive erasable capsule walls.<sup>7</sup> In addition to functions previously proposed for electrostatically assembled capsules, such as microcontainers,<sup>8–11</sup> microreactors,<sup>12,13</sup> or stimuli-responsive microcarriers,<sup>14,15</sup> hydrogen-bonded capsules also can serve as containers for fast pH-sensitive release of the container contents when needed. For certain biomedical applications, when stability of a polymeric wall at physiological pH is required, a microcontainer wall can be chemically cross-linked to provide desired stabilization.<sup>7,16</sup> Specifically, we have recently applied carbodiimide chemistry<sup>7</sup> to covalently cross-link hydrogen-bonded capsules in aqueous solution. Note that other routes of cross-linking hydrogen-bonded multilayers, such as thermal and photo-cross-linking, developed by Rubner and co-workers for planar films,<sup>17</sup> have limitations for cross-linking of polymer capsules dispersed in

water. Chemically cross-linked hydrogen-bonded capsules have recently shown much promise for biomedical applications as they have been demonstrated to exhibit resistance toward cell adhesion.<sup>16</sup> It should be also noted that deposition of hydrogen-bonded multilayers onto colloidal particles has been earlier demonstrated by Zhang et al.<sup>18</sup> for nonaqueous solutions, but the resulting films were not designed to be pH-responsive or to swell at physiological pH.

There are several fundamental features distinguishing hydrogen-bonded films from more widely used electrostatically associated polymer multilayers. One distinction is the reverse effect of hydrogen bonds and electrostatic interactions on internal ionization of self-assembled weak polyelectrolytes. When a weak poly(carboxylic acid) is self-assembled with a polycation, a significant increase of the polyacid ionization occurs due to extensive electrostatic pairing, usually described as a lowering of the solution p*K*<sub>a</sub>.<sup>19–22</sup> In contrast, hydrogen-bonding interactions stabilize the protonated form of a carboxylic group, resulting in suppression of ionization of the polyacid embedded within the film.<sup>6</sup> Another fundamental distinction is that, unlike electrostatic self-assembly, hydrogen-bonding is not driven by a charge-compensation mechanism, and electric charge of the same sign can be introduced within the films during film composition.<sup>23</sup> The latter films are only stable as long as unfavorable electrostatic repulsions are overcompensated by hydrogen bonding, and high charge density in the polyelectrolyte chains results in film instability.<sup>4,6</sup> The stability of hydrogen-bonded self-assembly has been studied in these systems when charges were introduced by a change of the solution pH at the post-assembly

step,<sup>6</sup> and the occurrence of an upper critical ionization was found above which self-assembled multilayers decomposed. More recently, Hammond and co-workers systematically studied the effect of the deposition pH on self-assembly of poly(ethylene oxide) (PEO) with poly(carboxylic acid)s and found that self-assembly is dramatically inhibited above a certain pH value when ionization of poly(carboxylic acid)s is increased.<sup>24</sup> Note that for electrostatically driven multilayer deposition an opposite trend is observed; i.e., a lower critical charge density exists below which the multilayers are not stable.<sup>25–27</sup>

In this paper, we discuss the effect of substrate charge on the deposition of hydrogen-bonded multilayers when the self-assembly pH is kept constant. Using a system involving hydrogen-bonding self-assembly that involves a weak poly(carboxylic acid), we demonstrate that substrate charge and the adsorption conditions of the precursor layers play a critical role in deposition of hydrogen-bonded films and that hydrogen-bonded film growth may be inhibited when a conformation of precursor-bound adsorbed weak polyacid provides a prohibitively strong electrokinetic potential at the surface. We discuss and contrast this effect using two systems with significantly different strengths of hydrogen bonding, i.e., strongly associating PVPON/PMAA and weakly associating PEO/PMAA films, and we suggest ways to initiate hydrogen-bonded self-assembly on substrates of various surface charge by various surface-priming strategies. We also present a comparative study of the deposition of hydrogen-bonded multilayers on flat and particulate substrates.

## Experimental Section

**Materials.** Poly(methacrylic acid) (PMAA;  $M_w$  150 000), poly(ethylene imine) (PEI;  $M_w$  600 000), poly(ethylene oxide) (PEO;  $M_w$  200 000), poly(*N*-vinylpyrrolidone) (PVPON;  $M_w$  55 000), calcium chloride, urea, hydrochloric acid, and sodium hydroxide were purchased from Sigma-Aldrich. Alexa Fluor 488 carboxylic acid succinimidyl ester fluorescent dye was obtained from Molecular Probes Inc. All chemicals were used without any further purification. Cadmium carbonate particles with an average diameter of 10  $\mu\text{m}$  were synthesized from urea and cadmium nitrate as described elsewhere.<sup>28</sup> Cadmium carbonate particles of about 1  $\mu\text{m}$  in size were produced by mixing equal amounts of 1 M cadmium nitrate and 1 M sodium carbonate solutions. The average size of produced  $\text{CdCO}_3$  particles was monitored by dynamic light scattering using a Malvern MasterSizer X particle size analyzer (Malvern Instruments Ltd.). The template particles of  $\text{SiO}_2$  were purchased from Polysciences Inc. as 10% dispersions in water and were of  $4.0 \pm 0.2 \mu\text{m}$  in diameter.

Millipore (Milli-Q system) filtered water with a resistivity 18.2 M $\Omega$  was used in all experiments.

**Preparation of Hydrogen-Bonded Capsules.** For all deposition steps, 0.2 mg/mL polymer solutions were used that allowed exposed surfaces to reach saturated adsorption conditions within a typical deposition time of 15 min. Hydrogen-bonded multilayers were deposited either on bare cadmium carbonate particles which carried a positive net surface charge or on PEI-coated  $\text{CdCO}_3$  particles. In the first case, the method included deposition of the PMAA from solution at pH = 6.5 followed by triple washing with buffer at pH = 3.5. Then PVPON/PMAA or PEO/PMAA layers were self-assembled at pH = 3.5. Each deposition cycle was followed by washing three times with a buffer solution at pH = 3.5 to remove excess polymer, followed by centrifugation of suspensions at 1200 rpm for 1 min to remove the supernatant. Deposition, washing, and redispersion steps were performed in a shaker (Fisher Scientific) at 1600 rpm.

In the second case, a precursor PEI layer was deposited onto  $\text{CdCO}_3$  surface using two routes. In route I, PEI was allowed to adsorb onto the surface of  $\text{CdCO}_3$  particles at pH = 3.5. In route II, PEI precursor was allowed to adsorb at a higher pH value of 6. Self-assembly of hydrogen-bonded layers was then performed at pH = 3.5, which started with the deposition of PMAA. The washing cycles were performed at the same conditions as described above.

In both cases, after a desired number of layers was deposited, the carbonate core was dissolved using 0.1 M HCl solution, yielding hollow polymeric capsules. Capsules were then repeatedly washed with 0.1 M HCl aqueous solution, using centrifugation as a means to separate capsules from the washing solution. Precipitation of hollow hydrogen-bonded capsules required higher centrifugation times and speeds as compared to separation of capsules coated on  $\text{CdCO}_3$  particles. We found that centrifugation at 5800 rpm for 30 min was required to precipitate ~90% of the hollow capsules with an average size of ~1  $\mu\text{m}$ .

**Microelectrophoresis.** All polymer solutions used for  $\zeta$ -potential measurements were prepared by dissolving the polymers in deionized water to produce 0.2 mg/mL solutions and subsequently adjusting pH with hydrochloric acid or sodium hydroxide. The deposition of polymers onto cadmium carbonate or  $\text{SiO}_2$  particles was monitored by laser microelectrophoresis technique using a Malvern Nano Zetasizer (Malvern Instruments Ltd.). Unless otherwise noted, 25  $\mu\text{L}$  of a 10% suspension of  $\text{CdCO}_3$  or  $\text{SiO}_2$  particles was repeatedly washed with deionized water and redispersed in 1 mL of water whose pH was adjusted to 3.5 with hydrochloric acid and used for  $\zeta$ -potential measurements. The results were averaged over 30 measurements.

**Fluorescence Optical Microscopy.** Fluorescence images of hydrogen-bonded capsules in solution were obtained on a Nikon Eclipse E1000 microscope with a 40xLU Plan objective lens. The multilayer capsules were visualized by dropping 10  $\mu\text{L}$  of the capsule solution on a glass slide and adding the Alexa Fluor 488 fluorescent dye for staining.

**Scanning Electron Microscopy (SEM).** SEM analysis was performed using a LEO 982 DSM instrument with a field-emission gun at an operation voltage of 1 or 5 kV. A drop of a particle suspension was applied either to a precleaned silicon wafer or a lacy-carbon copper TEM grid (Electron Microscopy Science), and measurements were conducted after specimens were allowed to dry for 2 h.

**Transmission Electron Microscopy (TEM).** TEM imaging was carried out using a Philips CM20 FEG transmission electron microscope at an operation voltage of 200 keV. Samples were prepared by applying a drop of a capsule solution onto a lacy-carbon gold TEM grid (Electron Microscopy Science), dried, and then analyzed. No staining was used for TEM measurements.

**Electron Energy-Loss Spectrometry (EELS).** EELS thickness measurements were carried out using the 200 keV Philips CM20 TEM with a Gatan 776 Enigma PEELS spectrometer. The microscope was operated in scanning-transmission (STEM) mode for these measurements. Hollow capsules were deposited from solution at pH = 1.0 onto a lacy-carbon gold TEM grid, dried, and cooled to  $-165^\circ\text{C}$ . The capsule wall thickness was derived at each point in a line scan across using the relation  $I_0 = I_{\text{total}} \exp(-t/\lambda)$ , where  $t$  is thickness,  $\lambda$  is the mean free path (MFP) for total inelastic electron scattering of the polymer,  $I_t$  is total and  $I_0$  the zero-loss electron intensity,<sup>29</sup> and  $\lambda = 260 \text{ nm}$  was based on independent measurements of polymers.

**ATR-FTIR Spectroscopy (ATR-FTIR).** In situ ATR-FTIR growth studies were done with a Bruker Equinox-55 Fourier transform infrared spectrometer equipped with a narrow-band mercury cadmium telluride detector. The experiments were performed at pH 3.5 using a home-built flow-through cell. The model PVPON/PMAA system was deposited onto a flat surface of oxidized Si. The oxidation of the surface, priming with the first layer, multilayer deposition, and calculation of the amount adsorbed have been previously described in the literature.<sup>30</sup>

**Atomic Force Microscopy (AFM).** The thickness measurements of the PVPON/PMAA films and capsules in a dry state were performed using a NanoScope IIIa scanning probe microscope in tapping mode (Digital Instruments, Veeco Metrology Group) employed Veeco Nanoprobe tips. The sample was prepared by applying 8  $\mu$ L of the capsule solution to a freshly cleaned mica surface and drying for 2 h in air. The capsule single wall thickness was determined as half of the height of the collapsed flat regions of dried capsules.

**Ellipsometry.** Thickness measurements of PEI/PMAA films were done using a custom-made phase-modulated ellipsometer. Before film deposition, silicon wafers were first sonicated in a mixture of 1 part of deionized water (DI) and 3 parts of 2-propanol for 15 min. After triple washing in DI water they were boiled at 70  $^{\circ}$ C in a 1:1:5 solution of hydrogen peroxide:ammonium hydroxide:DI water over 15 min. Washings in DI water followed. Samples were dried under a stream of nitrogen and then measured.

## Results and Discussion

**Deposition on Flat vs Particulate Substrates.** We have recently shown that hydrogen-bonded multilayers can be deposited on the surface of inorganic crystals such as cadmium carbonate particles.<sup>7</sup> The specific protocol included priming the surface of  $\text{CdCO}_3$  crystals (which carried positive charge in water when freshly prepared) with a layer of weak polyacid followed by deposition of hydrogen-bonded multilayers at pH 3.5. In this paper, we use different ways of priming the substrate surface, and we contrast the deposition of hydrogen-bonded multilayers onto particulate and flat surfaces using several complementary techniques. Specifically, EELS and AFM were applied to measure the thicknesses of hydrogen-bonded capsules, and ATR-FTIR and AFM were used for monitoring the film deposition onto a flat substrate. ATR-FTIR was used for measurements of in situ film deposition from  $\text{D}_2\text{O}$  solutions, while the other techniques all used films and capsules which were dried prior to measurements. Two types of colloidal particles were used as substrates, specifically  $\text{CdCO}_3$  or silica. Note that the latter carry the same surface chemical groups as the oxidized silicon wafers used as flat substrates in this study. To enhance the adhesion of hydrogen-bonded multilayers to oxidized surfaces of silicon crystals or to surfaces of  $\text{CdCO}_3$ , poly(ethylene imine) (PEI) was preadsorbed at these surfaces.

The top panel in Figure 1 shows the results of PVPON/PMAA capsule wall thickness measurements obtained with EELS and AFM. Although EELS has been earlier applied to obtain vibrational fingerprinting features of small organic molecules adsorbed on a solid surface,<sup>31</sup> we are not aware (apart from our earlier short communication<sup>7</sup>) of other work where EELS has been applied to quantify the thickness of self-assembled capsules made from organic polymers. Capsule wall thicknesses derived from EELS measurements were in remarkably good agreement with more commonly used AFM measurements<sup>32</sup> of the film thickness. The film deposition onto a flat substrate is illustrated in the bottom panel in Figure 1, showing consistent film thicknesses derived from two different techniques, i.e., AFM of the dry sample and in situ ATR-FTIR. When comparing the PVPON/PMAA film deposition onto the substrates of the two different geometries, a significant difference in the overall film growth is observed. While linear film growth was observed on the flat substrate until the number of layers was as high as 60, the linearity in polymer deposition onto particulate sub-

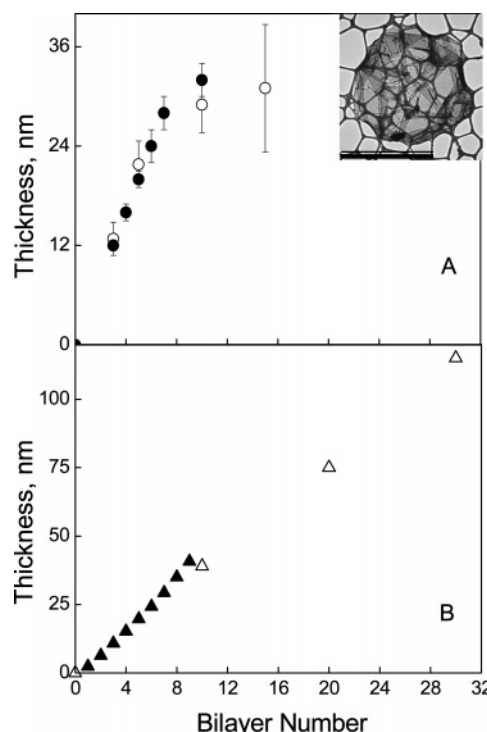


**Figure 1.** Top panel: the single wall thickness of dried hollow PVPON/PMAA capsules prepared on  $\text{CdCO}_3$  particles pre-coated with PEI at pH 3.5 and measured by EELS (open circles) and hollow PVPON/PMAA capsules grown on  $\text{SiO}_2$  microspheres at pH 2 without any precursor and analyzed using AFM (filled circles). The inset shows a typical TEM image of the dried  $(\text{PEI/PMAA})(\text{PVPON/PMAA})_n$  capsules after dissolution of the  $\text{CdCO}_3$  template. The scale bar is 8  $\mu\text{m}$ . Bottom panel: the thickness of PVPON/PMAA multilayers deposited on a flat oxidized silicon crystal and measured by in situ ATR-FTIR (filled triangles) and PVPON/PMAA dry multilayers deposited on silicon wafers at pH 2 (starting from PVPON) and measured by AFM (open triangles).

strates persisted only to the layer number 14, followed by a decrease in the amount of polymer adsorbed at each deposition step. We suggest that inhibition of the multilayer growth on a particulate substrate results from shaking of colloidal dispersions during polymer deposition and particle redispersion steps. It is reasonable to assume that chain removal is induced by shear and is facilitated for a thicker polymer coating.

It is also evident in Figure 1 that for substrates of several different types, with or without a precursor layer, a roughly constant amount of polymer ( $\sim 3.8$  nm) was deposited within a bilayer of PVPON/PMAA film when the number of layers deposited was smaller than 14. This illustrates the absence of the substrate templating effect on the amount of hydrogen-bonded polymers deposited within the film—an effect similar to that earlier found for electrostatically self-assembled multilayers.<sup>1</sup>

As illustrated above, the use of a positively charged precursor layer was not necessary when a bare surface carried positive charges, as in the case of freshly prepared  $\text{CdCO}_3$  particles.<sup>7</sup> We have found that  $\text{CdCO}_3$  particles prepared as described elsewhere<sup>28</sup> have a  $\zeta$ -potential of +15 to +25 mV while exposed to pH = 3.5 (0.0015 M HCl solution) and used within 1 day after the particle preparation. Both PVPON/PMAA and PEO/PMAA could be deposited onto this substrate at pH 3.5 using the polyacid priming layer. However, Figure 2 illustrates that the uniformity and the thickness of PEO/



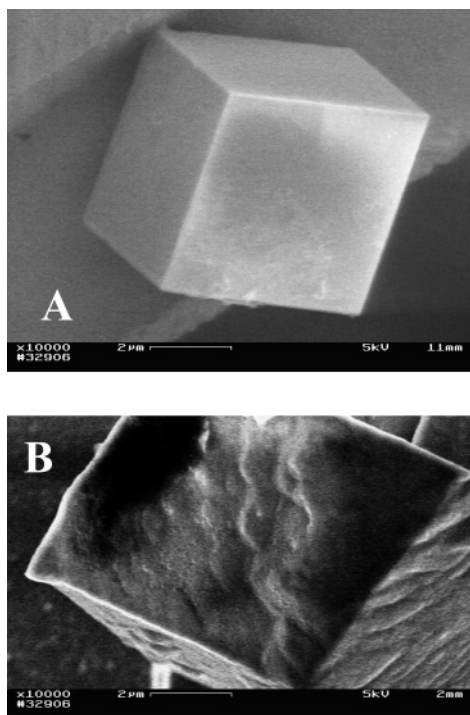


**Figure 2.** SEM images of  $\text{CdCO}_3$  template particles with  $(\text{PVPON/PMAA})_5$  (panel A) and  $(\text{PEO/PMAA})_5$  (panel B) coatings obtained via priming the positively charged template with PMAA.

PMAA and PVPON/PMAA multilayers coated onto the  $\text{CdCO}_3$  particles are clearly different. SEM images of dried PEO/PMAA multilayers on  $\text{CdCO}_3$  substrates indicate that the surface of  $(\text{PEO/PMAA})_5$ -coated particles is rough and that the film irregularity severely increases with the layer number. TEM imaging indicates that, after dissolution of  $\text{CdCO}_3$  core, dried PEO/PMAA capsules have highly inhomogeneous and possibly phase-separated capsule walls. This effect increases in dry PEO/PMAA films with increased number of deposited layers to the point that we were unable to reliably study the system growth because of high variability of thickness along the capsule wall. Interestingly, we did not observe these effects to the same extent in our previous TEM studies of PEO/PMAA on submicron-sized  $\text{CdCO}_3$  particles, and we attribute this to a significant difference in length scale over which phase separation develops. Note that phase separation in dry PEO/PMAA capsules probably does not reflect the morphology of highly hydrated PEO/PMAA capsules suspended in water. In contrast, a 10-layer PVPON/PMAA coating remains relatively smooth. When suspended in water, hollow  $(\text{PVPON/PMAA})_5$  capsules have a distinctive shape characteristic of the template particles (inset in Figure 3). When dried, PVPON/PMAA hollow capsules exhibit folds (see inset in Figure 1) similar to those found in electrostatically deposited polymer capsules.<sup>32</sup>

We have also found that while multilayers could be deposited onto inorganic particles whose charge was positive, no multilayers could be deposited onto the same inorganic template particles when they were dried before deposition and consequently acquired negative charge. We have also observed that the  $\zeta$ -potential of  $\text{CdCO}_3$  particles was not stable, and particles became negatively charged within the range of pH from 3.5 to 8.5 after they were stored for 2 weeks in water. This charge switch in inorganic carbonate salts as a result

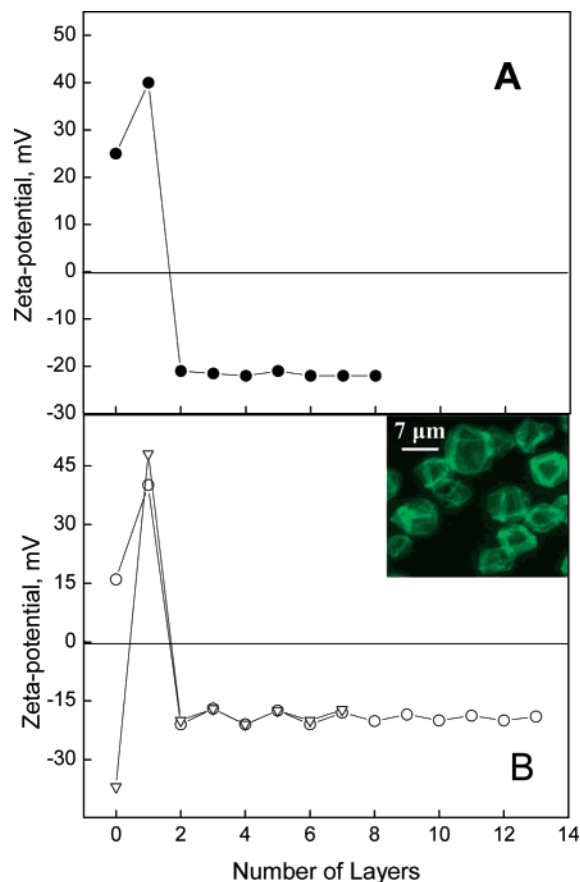


**Figure 3.**  $\zeta$ -potential variations of  $\text{CdCO}_3$  particles, initially negatively or positively charged (triangles or circles, respectively) during priming the surface with PEI precursor (layer number 1) and following deposition of PEO/PMAA (A) or PVPON/PMAA multilayers (B). Even layer numbers correspond to deposition of PMAA, and odd layer numbers reflect treatment with PEO (A) or PVPON (B). All deposition solutions contained 0.2 mg/mL of polymers at pH = 3.5. The inset shows a fluorescent image of hollow  $(\text{PEI/PMAA})(\text{PVPON/PMAA})_4$  capsules produced by cadmium carbonate core dissolution.

of preparation, storage, and drying has been observed<sup>33</sup> and is attributed to the hydrolysis of surface ions and adsorption of potential-determining ionic species at the crystal surface.<sup>34</sup> In our case, the  $\text{CdCO}_3$  suspension stored in aqueous solution under an ambient atmosphere for 3 weeks gave a  $\zeta$ -potential of  $-35$  mV at pH = 3.5, probably due to the adsorption of  $\text{HCO}_3^-$  and  $\text{CO}_3^{2-}$  ions at the crystal surface. Obviously, the resulting negative charge at the surface of  $\text{CdCO}_3$  inhibited deposition of the first PMAA layer performed at pH 6.5 because of electrostatic repulsion between the surface and the polyacid whose  $\text{pK}_a$  is  $\sim 6.5$ .<sup>6</sup> The inhibition of PVPON/PMAA multilayer deposition onto  $\text{CdCO}_3$  particles with the bare surface charge of  $-35$  mV was reflected by no changes in  $\zeta$ -potential observed when particles were sequentially brought into contact with PVPON and PMAA solutions and was confirmed by fluorescence optical microscopy and TEM imaging, both of which showed no evidence for capsule formation. Note that in the case of electrostatically associated films such inhibition is usually not observed since the substrate surface is brought into contact with solutions of positively and negatively charged polymer chains in an alternating way, and one of the two polymers adheres to the surface as a result of electrostatic attraction.

**The Role of a Precursor Layer.** In hydrogen-bonded self-assembly, the use of precursor layers such

**Table 1. Fabrication of PEO/PMAA and PVPON/PMAA Capsules on Bare CdCO<sub>3</sub> Substrates and on the Same Substrates Treated with PEI Using Routes I (PEI Deposited at pH 3.5) and II (PEI Deposited at pH 6)<sup>a</sup>**

$\zeta$ -potential of bare CdCO <sub>3</sub> particles at pH = 3.5	$\zeta$ -potential (at pH = 3.5) after PEI deposition using route I	$\zeta$ -potential (at pH = 3.5) after PEI deposition using route II	$\zeta$ -potential (at pH = 3.5) after deposition of the first PMAA layer	PEO/PMAA deposition at pH 3.5	PVPON/PMAA deposition at 3.5
+25 mV	+40 mV		-22 mV	no capsules	capsules
+25 mV		+48 mV	-1 mV	capsules	capsules

<sup>a</sup> All data are given for solutions whose pH was 3.5.

as PEI provides several advantages. First, in the case of a negatively charged substrate, deposition of a PEI layer reverses the surface charge and can provide enhanced adhesion of the hydrogen-bonded multilayer. In addition, PEI is known to strongly adsorb onto a majority of surfaces regardless of their charge, probably due to strong nonelectrostatic contributions to the adsorption energy.<sup>35,36</sup> This allows the use of PEI as an almost universal priming layer that eliminates many of the uncertainties associated with the poorly defined surface charge of inorganic particles or other encapsulated materials.

As already described in the Experimental Section, we have used two routes to deposit polycation precursor layers. These differed in the deposition pH chosen for the PEI adsorption and was pH = 3.5 in route I and pH = 6 in route II. Based on the  $pK_a$  of PEI of 8.8,<sup>37</sup> in both cases the PEI chains were positively charged due to protonation of amino groups. Adsorption of all subsequent layers was performed at pH 3.5.

Figure 3 illustrates the evolution of  $\zeta$ -potential during the deposition of PEO/PMAA and PVPON/PMAA multilayers onto CdCO<sub>3</sub> particles when route I of priming the surface with PEI was used. One can see that, regardless the charge of the bare CdCO<sub>3</sub> particles, adsorption of PEI affords a high density of positive charge to the surface. Specifically, even when the particle surface charge started positive (in the range of +15 to +35 mV), the addition of PEI further increased this surface charge to  $\zeta$ -potentials of +35 to +50 mV, confirming the binding of PEI to the already positively charged surface of the CdCO<sub>3</sub> particles. However, the PEI adhesion layer had different effects on the growth of PEO/PMAA and PVPON/PMAA films. Table 1 shows that, as observed by fluorescence microscopy of dye-stained capsules, PVPON/PMAA films were successfully deposited on the substrates of all types, but no PEO/PMAA capsules were produced when route I (adsorption of PEI at pH 3.5) was used for priming the surface.

This point is also seen in Figure 3, which compares  $\zeta$ -potential variations that accompanied multilayer deposition. The observation of no changes in  $\zeta$ -potential of PEI-treated CdCO<sub>3</sub> particles during alternating cycles of PEO/PMAA deposition (panel A in Figure 3) was consistent with the inhibition of the film growth. In contrast, evolution of  $\zeta$ -potential during deposition of PVPON/PMAA films onto PEI-treated particles corresponds to coating of cadmium carbonate particles with hydrogen-bonding multilayers (panel B in Figure 3).

With application of route II for PEI adsorption, no inhibition of growth of hydrogen-bonded multilayers occurred in both systems (Table 1). This effect will be discussed in the next section.

Specific changes in  $\zeta$ -potential of CdCO<sub>3</sub> particles which accompany growth of hydrogen-bonded capsules deserve more detailed discussion. As shown in Table 1 and Figure 3, the  $\zeta$ -potential of CdCO<sub>3</sub> particles reversed its sign after adsorption of a PMAA layer (layer

2 in Figure 3B) at pH = 3.5. The reversal of surface charge is a typical feature of electrostatic self-assembly of polyelectrolytes and is usually observed during deposition of oppositely charged polymers at surfaces.<sup>38</sup> However, starting from the neutral polymer layer (layer 3), when self-assembly was continued through hydrogen bonding, the net surface charge remained negative, and the  $\zeta$ -potential oscillated between negative values which differ by a small but highly reproducible value of  $\sim 5$  mV in the PVPON/PMAA system (Figure 3B). Note that deposition of PEO/PMAA multilayers onto positively charged surfaces of bare CdCO<sub>3</sub> particles was also accompanied by changes in  $\zeta$ -potential but with larger ( $\sim 10$  mV) variation in amplitude (Figure 4). It is interesting that during hydrogen-bonding self-assembly, in contrast to electrostatic self-assembly, there was no surface-charge reversal, and the negative charge of the surface could be maintained throughout the entire self-assembly process, thus preventing particle aggregation. Similar oscillations of  $\zeta$ -potential were recently observed by Rubner and co-workers<sup>16</sup> during hydrogen-bonded self-assembly of poly(acrylic acid)/poly(acrylamide) (PAA/PAam) on colloidal particles but with a larger amplitude of the  $\zeta$ -potential variations. The differences in the amplitude of  $\zeta$ -potential oscillations during self-assembly of hydrogen-bonded polymers in different systems most probably result from the thickness of adsorbed neutral polymers on the electrophoretic mobility of colloidal particles. When uncharged polymer adsorbs onto a charged surface, the effective slip plane at which electrophoretic mobility (and  $\zeta$ -potential) is measured moves away from the solid surface due to hydrodynamic immobilization of water associated with the polymer loops.<sup>39</sup> A specific value of  $\zeta$ -potential lowering then depends on the amount of neutral polymer adsorbed and on the structure of the adsorbed layer. Weaker polymer binding results in more fluffy conformations of adsorbed

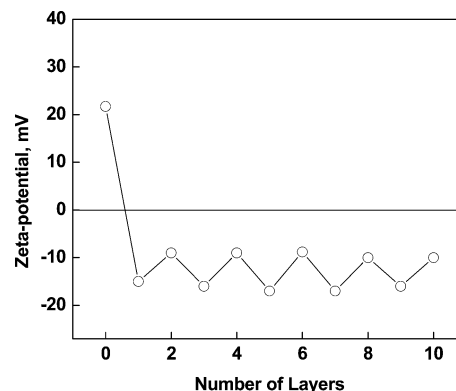


**Figure 4.**  $\zeta$ -potential variations during deposition of PEO/PMAA on bare positively charged CdCO<sub>3</sub> particles at pH 3.5. Layer 1 corresponds to the  $\zeta$ -potential of CdCO<sub>3</sub> substrate coated with PMAA layer deposited at pH 6.5 and subsequently washed with water with pH 3.5 three times. Odd layer numbers correspond to deposition of PMAA, and even layer numbers reflect treatment with PEO. All deposition solutions contained 0.2 mg/mL of polymers at pH = 3.5.

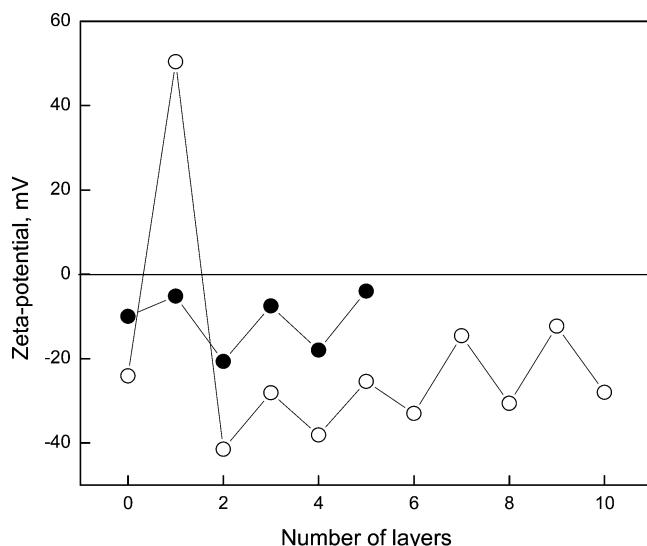


**Figure 5.** Alternations of  $\zeta$ -potential of PEO/PMAA deposited on bare  $\text{SiO}_2$  particles (filled circles) and PEI-pretreated (open circles) at pH 3.5. Layer number one corresponds to the  $\zeta$ -potential of  $\text{SiO}_2$  substrate coated with PEO (filled circles) or PEI (open circles) layers at pH 3.5. Layer 2 illustrates deposition of PMAA from 0.2 mg/mL solution at pH = 3.5, and the further steps correspond to alternative deposition of PEO and PMAA from water solutions at pH 3.5.

chains, larger amounts of polymer adsorbed, and larger shifts of the slip plane in solution. In our previous publication,<sup>6</sup> we found that the amount of PEO deposited per layer is larger than that of PVPON when these polymers are self-assembled with poly(carboxylic acid)s due to weaker binding of PEO with the polyacid. This is consistent with our observation of larger-amplitude  $\zeta$ -potential alternations for the PEO/PMAA system (Figure 4).

It is also interesting that when a different substrate— $\text{SiO}_2$  particles—was used for multilayer deposition, addition of PEO and PMAA solutions to both bare negatively charged particles or to particles which were treated with PEI using route I resulted in  $\zeta$ -potential variations (see Figure 5) similar to those seen in Figure 4 for  $\text{CdCO}_3$  substrates. However, as was proved by fluorescence and TEM imaging, no capsules were produced under these conditions. It is likely that observed  $\zeta$ -potential variations reflect hydrogen bonding of PEO with protonated silanol groups of  $\text{SiO}_2$  which are abundant at pH 3.5. Subsequent exposure to PMAA then removes PEO to free complexes in solution. Both the weak binding of PEO to the  $\text{SiO}_2$  surface and shaking the particle suspension during polymer deposition steps are likely to assist polymer-chain removal.

**Rationalization of the Effect of Different Routes of PEI Adsorption on Hydrogen-Bonded Self-Assembly.** Our discussion in this section is focused on contrasting the effect of the substrate on the growth of weak polyelectrolyte hydrogen-bonding multilayers. These effects can be rationalized by considering the different structure of weak polyelectrolyte layers induced by a precursor-coated solid surface with variable charge density. We argue that substrates of different charge can produce polyacid layers with more or less heterogeneous structure which strongly affect the electrokinetic potential of the surface and its propensity to support hydrogen-bonded film growth.

The two routes of priming the surface with PEI differ in the pH value used for PEI adsorption. Measurements

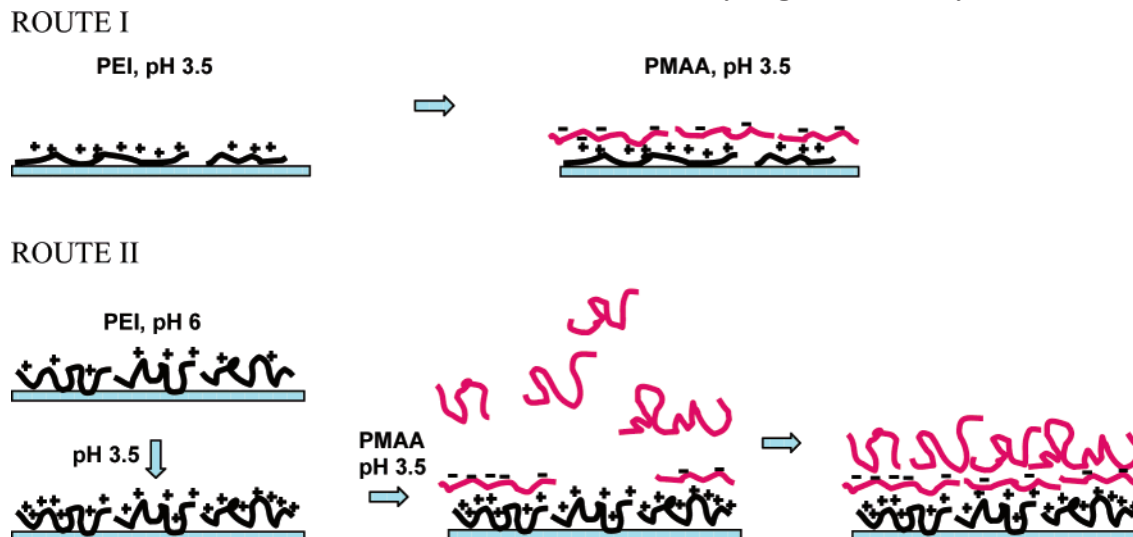
of  $\zeta$ -potential of bare  $\text{CdCO}_3$  particles which carry either positive or negative charge at pH = 3.5 showed that for the particles of both types the surface charge became more negative with an increase in pH (data not shown). Note that a similar increase in the negative surface-charge density at high pH is observed with substrates carrying silanol groups such as the surface of a silicon wafer or silica particles. Since it was not possible to measure the amount of PEI adsorbed onto  $\text{CdCO}_3$  substrates in our experiment, we have studied the pH dependence of PEI binding at a model surface of oxidized silicon wafers. It was earlier shown that the amount of PEI adsorbed onto a silica surface increases with increasing pH.<sup>36</sup> As shown by our ellipsometry measurements of the amounts of PEI deposited within a precursor layer using routes I and II, significantly more PEI was adsorbed onto a surface of oxidized silicon wafer in route II when a high pH value was used for deposition (1 nm vs 2.5 nm for routes I and II, respectively, with an experimental error of 0.2 nm). Further deposition of PMAA under route II conditions roughly doubled the PMAA layer thickness (0.8 nm vs 2 nm for routes I and II, respectively). Using in situ ATR-FTIR and quantification of  $-\text{COOH}$  and  $-\text{COO}^-$  bands described earlier,<sup>6,21–23</sup> we have also shown that PMAA chain ionization was 6% vs 8% for routes I and II of PEI deposition, respectively, with a statistically valid error of 1%. We rationalize these findings on the basis of the higher surface charge density provided by the PEI chains when route II is used and the further dependence of PMAA ionization on the substrate charge density. Specifically, two points differentiate adsorption of PEI at high pH from its binding at lower pH (Table 2). First, when PEI is adsorbed on  $\text{SiO}_2$  particulate substrates at pH 6, larger amounts of polyelectrolyte are brought to the surface because of the increased density of negative charge. This line of argument is consistent with common theoretical and experimental observations for the adsorption of polyelectrolyte chains driven by a charge-compensation mechanism<sup>40,41</sup> Second, adsorbed PEI chains are expected to have a lower linear charge density because of deprotonation of secondary and tertiary amine groups at pH = 6. PEI chains consequently adopt a more loopy surface conformation. As Table 2 shows, these two factors result in a much higher value of  $\zeta$ -potential of template particles after the ambient pH is changed to 3.5 and more amino groups acquire charge. Note also that the variation in pH from 6 to 3.5 reduces the amount of negatively charged silanol groups at the surface. We observed similar difference in routes I and II of PEI deposition onto  $\text{CdCO}_3$  substrates (see Table 1).

The larger charge of the PEI-treated surface obtained in route II has a double effect on the subsequently adsorbed PMAA chains. First, it explains the larger average ionization of the polyacid chains of ~8%. The adjustment of weak polyelectrolyte ionization within a single adsorbed layer has been theoretically predicted by Böhmer et al.<sup>42,43</sup> and also found experimentally.<sup>44,45</sup> In the case of electrostatically assembled films, similar local electrostatic effects result in lowering the  $\text{pK}_{\text{a}}$ s of weak self-assembled polyacids<sup>19–22</sup> as discussed above. We have also reported earlier that ionization of a weak polyacid within the polyelectrolyte multilayers increases with the polycation charge density.<sup>21</sup> Our current observation is in good agreement with these earlier findings. We then argue that the second effect of the



**Table 2. Fabrication of PEO/PMAA Capsules on the SiO<sub>2</sub> Substrate Using Routes I and II**

$\zeta$ -potential of bare SiO <sub>2</sub> particles at pH = 3.5 (top) and pH = 6 (bottom)	$\zeta$ -potential (at pH = 3.5) after PEI deposition using route I	$\zeta$ -potential (at pH = 3.5) after PEI deposition using route II	$\zeta$ -potential (at pH = 3.5) after deposition of the first PMAA layer	PEO/PMAA deposition at pH 3.5	PVPON/PMAA deposition at pH 3.5
−24 mV −49 mV	+50 mV	+69 mV	−42 mV −1 mV	no capsules capsules	capsules capsules

**Scheme 1. Schematic Representation of Routes I and II, the Precursor Layers, and Their Effect on Conformation of PMAA and Further Growth of Hydrogen-Bonded Layers<sup>a</sup>**

<sup>a</sup> Heterogeneous PMAA adsorbed layers produced in route II resulting into low values of surface  $\zeta$ -potential and promote further growth of hydrogen-bonded PEO/PMAA films.

high density of positive charge provided in route II is on the structure of the PMAA layer. We thus turn our attention to the effect of surface crowding on polymer-chain conformation during polymer adsorption. Specifically, we hypothesize that a high positive-charge density results in a high local density of PMAA chains adsorbed at the surface at pH 3.5. In this situation, the adsorbed-layer heterogeneity becomes prominent, and when PMAA chains reach a surface with high positive-charge density, chains that first arrive at the surface become highly flattened and highly ionized while later-arriving chains are forced to adopt more fluffy conformations because many adsorption sites are already occupied. This scenario is illustrated in Scheme 1. Although a fraction of polymer chains that adopt more extended conformations could be small, these chains efficiently determine the hydrodynamic layer thickness and shift the slip plane further away from the surface, resulting in a lower value of surface  $\zeta$ -potential. Polymer segments of PMAA chains which extend far from the charged surface will be less ionized and consequently will promote the further adhesion of PEO and growth of a PEO/PMAA multilayer. In our earlier publication,<sup>6</sup> we confirmed the occurrence of a critical ionization degree of PMAA, above which hydrogen-bonded multilayers are not stable, and this finding suggests that ionization of PMAA loops should not exceed about ~4% for the subsequent deposition of a PEO/PMAA multilayer to occur. The concept of an inhomogeneous structure of adsorbed layers suggested for route II of PEI deposition and shown in Scheme 1 is consistent with earlier experimental findings of conformational inhomogeneity of adsorbed polymer layers.<sup>44,46–48</sup> Structural inhomogeneity has also been suggested as a means to increase the surface binding energy and the polymer chain stiffness as in the case of polyelectrolytes.<sup>49,50</sup> Our

model of larger inhomogeneity of adsorbed layers is consistent with these observations and reflects a slowing structural reorganization of the adsorbed chains as the number of sticking points per chain (as reflected by increased PMAA ionization) increases.

Though we were able to produce (PEI/PMAA)(PEO/PMAA)<sub>2</sub> capsules onto CdCO<sub>3</sub> substrate using deposition route II, these capsules had a high propensity for coagulation, which we attribute to their low electrokinetic potential.

**Two Ways To Promote Growth of Hydrogen-Bonded Multilayers. 1. Hybrid PVPON/PEO/PMAA Capsules.** The high sensitivity of PEO/PMAA self-assembly to the substrate charge is a consequence of weak intermolecular bonding between PEO and PMAA.<sup>6,51</sup> More strongly interacting PVPON/PMAA chains have a higher PMAA critical ionization to inhibit subsequent PVPON/PMAA multilayer growth, and thus the deposition of these hydrogen-bonded multilayers occurs on both substrates (on CdCO<sub>3</sub> via routes I and II). One can take advantage of these differences by growing composite films where the substrate charge is manipulated by first depositing PVPON/PMAA and subsequently depositing PEO/PMAA. Intermediate PVPON/PMAA layers can be deposited onto PEI-coated CdCO<sub>3</sub> substrate that screen the surface charge and allow further adhesion of PEO/PMAA multilayers. We have found that using only one PVPON/PMAA bilayer was sufficient to ensure further deposition of a PEO/PMAA film. Figure 6 shows a fluorescence image of hybrid capsules. Considering that (PEI/PMAA)/(PVPON/PMAA) capsules were unstable upon core dissolution unless at least three PVPON/PMAA bilayers were deposited, the fact that (PEI/PMAA)/(PVPON/PMAA)/(PEO/PMAA)<sub>3</sub> stable hybrid capsules were produced proves the deposition of PEO/PMAA layers. As seen in

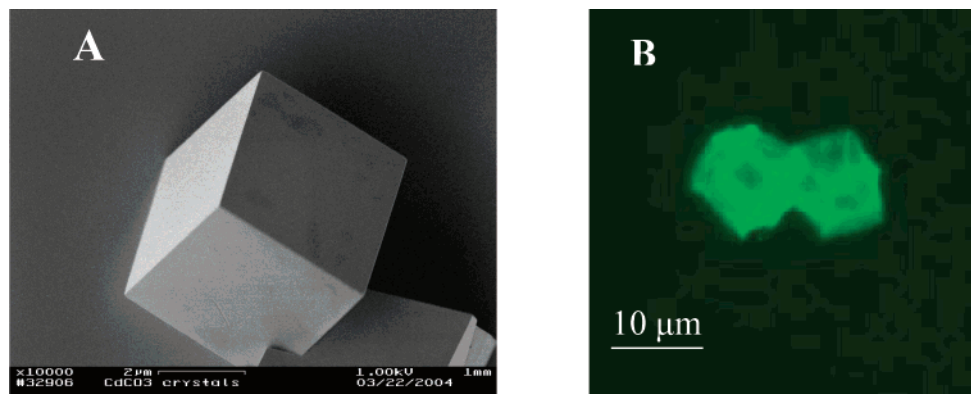


**Figure 6.** SEM images of a bare cadmium carbonate template particle (scale bar is 2  $\mu\text{m}$ ) (panel A) and a fluorescence microscope image of hollow (PEI/PMAA)/(PVPON/PMAA)/(PEO/PMAA)<sub>3</sub> hybrid hydrogen-bonded capsules (panel B) after core dissolution.

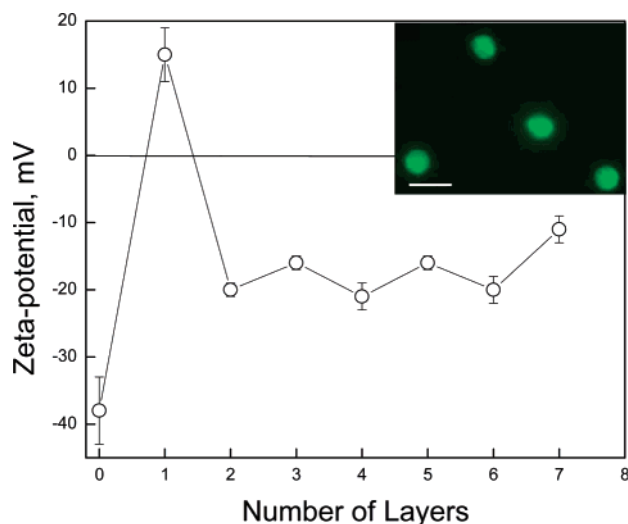


**Figure 7.**  $\zeta$ -potential variations of cadmium carbonate particles in the process of  $\text{Ca}^{2+}$ -assisted deposition of PVPON/PMAA multilayers. Layer 1 corresponds to the  $\zeta$ -potential of  $\text{CdCO}_3$  substrate in the presence of 0.02 M  $\text{CaCl}_2$  solution. Odd layer numbers correspond to deposition of PVPON, and even layer numbers reflect treatment with PMAA. All deposition solutions contained 0.2 mg/mL of polymers at pH = 3.5. The inset shows a fluorescent image of (PMAA/PVPON)<sub>4</sub>PMAA hollow capsules produced through  $\text{Ca}^{2+}$ -assisted deposition of the multilayers on negatively charged  $\text{SiO}_2$  microspheres after core dissolution in HF. The scale bar corresponds to 8  $\mu\text{m}$ .

Figure 6, the capsules follow the shape of the  $\text{CdCO}_3$  template (rhombohedral crystals with an average diameter of 10  $\mu\text{m}$ ).

**2. The Use of  $\text{Ca}^{2+}$  Ions To Promote Multilayer Growth.** Binding of PMAA to a  $\text{CdCO}_3$  surface when the substrate surface is negatively charged can be enabled through “stitching” by divalent ions. Binding of negatively charged biomolecules, such as DNA, to silica surfaces in the presence of divalent cations ( $\text{Ca}^{2+}$ ,  $\text{Mg}^{2+}$ ) has been earlier described in the literature.<sup>52,53</sup> We used a similar procedure to induce adsorption of PMAA onto cadmium carbonate. Figure 7 shows that the initial negative charge of bare  $\text{CdCO}_3$  particles (−38 mV) switches sign (+15 mV) when HCl-adjusted water supernatant at pH 3.5 was replaced with 0.02 M  $\text{CaCl}_2$  solution. After a single centrifugation of  $\text{Ca}^{2+}$ -treated particles, followed by redispersing into a 0.2 mg/mL PMAA solution at pH = 6.5 and subsequent triple washing in water at pH 3.5, the  $\zeta$ -potential of coated particles reversed its sign, suggesting that PMAA adsorbed at the template surface under these conditions. Subsequent deposition of PVPON and PMAA resulted

into an alternation of the  $\zeta$ -potential similar to that discussed earlier. As proven by fluorescence microscopy and TEM imaging, capsules can be grown successfully after depositing at least three PVPON/PMAA bilayers. This route was also applied to strongly negatively charged  $\text{SiO}_2$  particles (with  $\zeta$ -potential of −24 mV at pH 3.5), and hydrogen-bonded (PMAA/PVPON)<sub>4</sub>PMAA capsules were successfully produced (inset in Figure 7). This method presents a different approach to growing H-bonded capsules onto negatively charged surfaces.

## Conclusion

In summary, we describe the effect of substrate charge and precursor adsorption history on the formation of hydrogen-bonded multilayers, and we find that a polycation critically affects the structure of the first adsorbed layer of a weak poly(carboxylic acid) and the subsequent film growth. The precursor layer effect is uniquely important for hydrogen-bonded self-assembly because growth can be inhibited when the segmental ionization of a weak polyacid exceeds a threshold value. We also demonstrate that this effect can be eliminated by modifying the deposition conditions for the PEI precursor layer or by producing hybrid PVPON/PEO/PMAA hydrogen-bonded capsules. In addition, we have demonstrated the possibility of direct PMAA deposition onto a negatively charged template in the presence of calcium ions under conditions where PMAA carries negative charges. The latter way can be used to promote growth of hydrogen-bonded capsules onto negatively charged surfaces in cases when the use of a polycation precursor layer is not desirable.

**Acknowledgment.** We thank Eugenia Kharlampieva for in situ ATR-FTIR measurements and valuable suggestions. This work was supported by the National Science Foundation (Award DMR-0209439), the American Chemical Society Petroleum Research Fund (Award #41576-AC7), and RESBIO—The National Resource for Polymeric Biomaterials (NIH NIBIB PH1 EB001046-01A1).

## References and Notes

- (1) Fisher, P.; Laschewsky, A.; Wischerhoff, E.; Arys, X.; Jonas, A.; Legras, R. *Macromol. Symp.* **1999**, *137*, 1.
- (2) Stockton, W. B.; Rubner, M. F. *Macromolecules* **1997**, *30*, 2717.
- (3) Wang, L. Y.; Fu, Y.; Wang, Z. Q.; Fan, Y.; Zhang, X. *Langmuir* **1999**, *15*, 1360.
- (4) Sukhishvili, S. A.; Granick, S. *J. Am. Chem. Soc.* **2000**, *122*, 9550.



- (5) Wang, L.; Cui, S.; Wang, Z.; Zhang, X. *Langmuir* **2000**, *16*, 10490.
- (6) Sukhishvili, S. A.; Granick, S. *Macromolecules* **2002**, *35*, 301.
- (7) Kozlovskaya, V.; Ok, S.; Sousa, A.; Libera, M.; Sukhishvili, S. *Macromolecules* **2003**, *36*, 8590.
- (8) Sukhorukov, G. B.; Antipov, A. A.; Voigt, A.; Donath, E.; Möhwald, H. *Macromol. Rapid Commun.* **2001**, *22*, 44.
- (9) Caruso, F.; Trau, D.; Möhwald, H.; Renneberg, R. *Langmuir* **2000**, *16*, 1485.
- (10) Diaspro, A.; Silvano, D.; Krol, S.; Cavalleri, O.; Gliozzi, A. *Langmuir* **2002**, *18*, 5047.
- (11) Volodkin, D. V.; Petrov, A. I.; Prevot, M.; Sukhorukov, G. B. *Langmuir* **2004**, *20*, 3398.
- (12) Shchukin, D. G.; Sukhorukov, G. B. *Langmuir* **2003**, *19*, 4427.
- (13) Antipov, A.; Shchukin, D.; Fedutik, Y.; Zhanaveskina, I.; Klechkovskaya, V.; Sukhorukov, G.; Möhwald, H. *Macromol. Rapid Commun.* **2003**, *24*, 274.
- (14) Glinel, K.; Sukhorukov, G.; Möhwald, H.; Khrenov, V.; Tauer, K. *Macromol. Chem. Phys.* **2003**, *204*, 1784.
- (15) Dejugnat, C.; Sukhorukov, G. B. *Langmuir* **2004**, *20*, 7265.
- (16) Yang, S. Y.; Lee, D.; Cohen, R. E.; Rubner, M. F. *Langmuir* **2004**, *20*, 5978.
- (17) Yang, S. Y.; Rubner, M. F. *J. Am. Chem. Soc.* **2002**, *124*, 2100.
- (18) Zhang, Y.; Guan, Y.; Yang, S.; Xu, J.; Han, C. *Adv. Mater.* **2003**, *15*, 835.
- (19) Mendelsohn, J. D.; Barrett, C. J.; Chan, V. V.; Pal, A. J.; Mayes, A. M.; Rubner, M. F. *Langmuir* **2000**, *16*, 5017.
- (20) Rmaile, H. J.; Schlenoff, J. B. *Langmuir* **2002**, *18*, 8263.
- (21) Kharlampieva, E.; Sukhishvili, S. A. *Langmuir* **2003**, *19*, 1235.
- (22) Izumrudov, V.; Sukhishvili, S. A. *Langmuir* **2003**, *19*, 5188.
- (23) Kharlampieva, E.; Sukhishvili, S. A. *Macromolecules* **2003**, *36*, 9950.
- (24) DeLongchamp, D. M.; Hammond, P. T. *Langmuir* **2004**, *20*, 5403.
- (25) Hoogveen, N. G.; Cohen Stuart, M. A.; Fleer, G. J.; Böhmer, M. R. *Langmuir* **1996**, *12*, 3675.
- (26) Steitz, R.; Jaeger, W.; Klitzing, R. *Langmuir* **2001**, *17*, 4471.
- (27) Glinel, K.; Moussa, A.; Jonas, A. M.; Laschewsky, A. *Langmuir* **2002**, *18*, 1408.
- (28) Janecovic, A.; Matijevic, E. *J. Colloid Interface Sci.* **1985**, *103*, 436.
- (29) Egerton, R. F. *Electron Energy-Loss Spectroscopy in the Electron Microscope*, 2nd ed.; Plenum Press: New York, 1996.
- (30) Izumrudov, V.; Kharlampieva, E.; Sukhishvili, S. *Biomacromolecules*, in press.
- (31) Sexton, B. A.; Avery, N. R. *Surf. Sci.* **1983**, *129*, 21.
- (32) Leporatti, S.; Voigt, A.; Mitlöhner, R.; Sukhorukov, G.; Donath, E.; Möhwald, H. *Langmuir* **2000**, *16*, 4059.
- (33) Chibowski, E.; Hotysz, L.; Szczes, A. *Colloids Surf., A* **2003**, *222*, 41.
- (34) Moulin, P.; Roques, H. *J. Colloid Interface Sci.* **2003**, *261*, 115.
- (35) Koper, G. J. M.; van Duijvenbode, R. C.; Stam, D. D. P. W.; Steuerle, U.; Borkovec, M. *Macromolecules* **2003**, *36*, 2500.
- (36) Meszaros, R.; Thompson, L.; Bos, M.; de Groot, P. *Langmuir* **2002**, *18*, 6164.
- (37) Amara, M.; Kerdjoudj, H. *Desalination* **2004**, *168*, 195.
- (38) Sukhorukov, G. B.; Donath, E.; Lichtenfeld, H.; Knippel, E.; Knippel, M.; Budde, A.; Möhwald, H. *Colloids Surf., A* **1998**, *137*, 253.
- (39) Koopal, L. K.; Lyklema, J. *Faraday Discuss. R. Soc. Chem.* **1975**, *59*, 230.
- (40) Fleer, G. J.; Cohen Stuart, M.; Scheutjens, J. M. H. M.; Cosgrove, T.; Vincent, B. *Polymers at Interfaces*; Chapman & Hall: London, 1993.
- (41) Dobrynin, A. V. *J. Chem. Phys.* **2001**, *114*, 8145.
- (42) Böhmer, M. R.; Evers, O. A.; Scheutjens, J. M. H. M. *Macromolecules* **1990**, *23*, 2288.
- (43) Cohen Stuart, M. A.; Fleer, G. J.; Lyklema, J.; Norde, W.; Scheutjens, J. M. H. M. *Adv. Colloid Interface Sci.* **1991**, *34*, 477 and references therein.
- (44) Hoogveen, N. G.; Cohen Stuart, M. A.; Fleer, G. J. *J. Colloid Interface Sci.* **1996**, *182*, 133.
- (45) Sukhishvili, S. A.; Chechik, O. S.; Yaroslavov, A. A. *J. Colloid Interface Sci.* **1996**, *178*, 42.
- (46) Sukhishvili, S. A.; Granick, S. *J. Chem. Phys.* **1998**, *109*, 6869.
- (47) Tanaka, H.; Swerin, A.; Ödberg, L. *Langmuir* **1994**, *10*, 3466.
- (48) Vandeven, T. G. M. *Adv. Colloid Interface Sci.* **1994**, *48*, 121.
- (49) Denoyel, R.; Durand, G.; Lafuma, F.; Audebert, R. *J. Colloid Interface Sci.* **1990**, *139*, 281.
- (50) Sukhishvili, S. A.; Granick, S. *J. Chem. Phys.* **1998**, *109*, 6861.
- (51) Abe, K.; Koide, M.; Tsuchida, E. *Macromolecules* **1977**, *10*, 1259.
- (52) Dederich, D. A.; Okwuonu, G.; Garner, T.; Denn, A.; Sutton, A.; Escotto, M.; Martindale, A.; Delgado, O.; Muzny, D. M.; Gibbs, R. A.; Metzker, M. L. *Nucleic Acids Res.* **2002**, *30*, 32.
- (53) Kumar, A.; Larsson, O.; Parodi, D.; Liang, Z. *Nucleic Acids Res.* **2000**, *28*, 71.

MA0501895